Continuous downstream processing of milled electrospun fibers to tablets monitored by near-infrared and Raman spectroscopy

Edina Szabó , Petra Záhonyi , Martin Gyürkés , Brigitta Nagy , Dorián L. Galata , Lajos Madarász , Edit Hirsch , Attila Farkas , Sune K. Andersen , Tamás Vígh , Geert Verreck , István Csontos , György Marosi , Zsombor K. Nagy

PII: S0928-0987(21)00208-6
DOI: https://doi.org/10.1016/j.ejps.2021.105907
Reference: PHASCI 105907

To appear in: *European Journal of Pharmaceutical Sciences*

Received date: 27 March 2021
Revised date: 30 April 2021
Accepted date: 7 June 2021

Please cite this article as: Edina Szabó , Petra Záhonyi , Martin Gyürkés , Brigitta Nagy , Dorián L. Galata , Lajos Madarász , Edit Hirsch , Attila Farkas , Sune K. Andersen , Tamás Vígh , Geert Verreck , István Csontos , György Marosi , Zsombor K. Nagy , Continuous downstream processing of milled electrospun fibers to tablets monitored by near-infrared and Raman spectroscopy, *European Journal of Pharmaceutical Sciences* (2021), doi: https://doi.org/10.1016/j.ejps.2021.105907

Highlights:

- Continuous feeding, blending and tableting of electrospun fibers was accomplished
- In-line monitoring of the amorphous solid dispersion content was performed
- The prepared tablets passed the USP <905> content uniformity test
- Continuous manufacturing of milled electrospun materials to tablets proved feasible

Continuous downstream processing of milled electrospun fibers to tablets monitored by near-infrared and Raman spectroscopy

Edina Szabó[1]; Petra Záhonyi[1]; Martin Gyürkés[1]; Brigitta Nagy[1], Dorián L. Galata[1]; Lajos Madarász[1]; Edit Hirsch[1]; Attila Farkas[1]; Sune K. Andersen[2]; Tamás Vígh[2]; Geert Verreck[2]; István Csontos[1]; György Marosi[1]; Zsombor K. Nagy[1*]

[1]Department of Organic Chemistry and Technology, Budapest University of Technology and Economics (BME), H-1111, Budapest, Műegyetem rakpart 3, Hungary

[2]Oral Solids Development, Janssen R&D, B-2340 Beerse, Turnhoutseweg 30, Belgium

**Corresponding author: Tel: +36 1463-1424; E-mail: zsknagy@oct.bme.hu*

Graphical Abstract

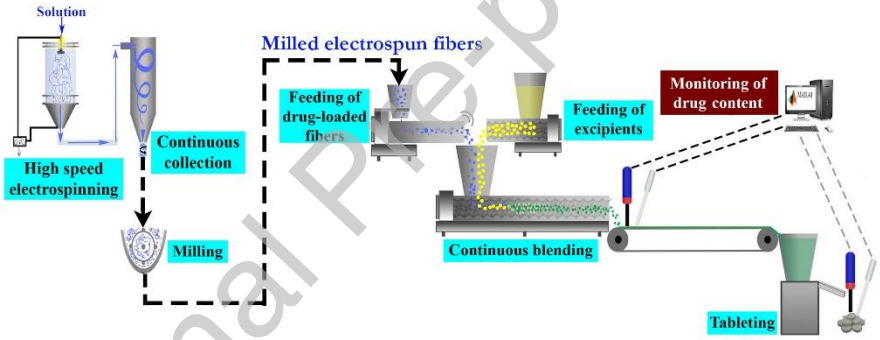

Abstract

Electrospinning is a technology for manufacture of nano- and micro-sized fibers, which can enhance the dissolution properties of poorly water-soluble drugs. Tableting of electrospun fibers have been demonstrated in several studies, however, continuous manufacturing of tablets have not been realized yet. This research presents the first integrated continuous processing of milled drug-loaded electrospun materials to tablet form supplemented by process analytical tools for monitoring the active pharmaceutical ingredient (API) content. Electrospun fibers of an amorphous solid dispersion (ASD) of itraconazole and poly(vinylpyrrolidone-*co*-vinyl acetate) were produced using high speed electrospinning and afterwards milled. The milled fibers with an average fiber diameter of 1.6 ± 0.9 µm were continuously fed with a vibratory feeder into a twin-screw blender, which was integrated with a tableting machine to prepare tablets with ~ 10 kN compression force. The blend of fibers and excipients leaving the continuous blender was characterized with a bulk density of 0.43 g/cm^3 and proved to be suitable for direct tablet compression. The ASD content, and thus the API content was determined in-line before tableting and at-line after tableting using near-infrared and Raman spectroscopy. The prepared tablets fulfilled the USP <905> content uniformity requirement based on the API content of ten randomly selected tablets. This work highlights that combining the advantages of electrospinning (e.g. less solvent, fast and gentle drying, low energy consumption, and amorphous products with high specific surface area) and the continuous technologies opens a new and effective way in the field of manufacturing of the poorly water-soluble APIs.

Keywords:

amorphous solid dispersion, electrospinning, scale-up, continuous formulation, process analytical technologies, tablets

Highlights:

- Continuous feeding, blending and tableting of electrospun fibers was accomplished
- In-line monitoring of the amorphous solid dispersion content was performed
- The prepared tablets passed the USP <905> content uniformity test
- Continuous manufacturing of milled electrospun materials to tablets proved feasible

1. Introduction

A large portion (up to 75%) of small molecule drug candidates in today's development portfolio has poor water solubility and is one of the main challenges in the pharmaceutical industry (Williams et al., 2013). Amorphous solid dispersions (ASDs) are a common technology and effective way to enhance the dissolution properties of poorly water-soluble molecules (Jermain et al., 2018; Pandi et al., 2020). Several techniques are known to prepare ASDs among which spray drying and hot-melt extrusion are the most typically used (Jermain et al., 2018; Pandi et al., 2020). However, electrospinning is also a very gentle and promising continuous method since it is capable of drying at ambient temperature and operates at atmospheric pressure (Yu et al., 2018). Furthermore, the energy consumption and the solvent needs during ES are favorable compared to the other solvent-based ASD preparation methods (Drosou et al., 2017; Kang et al., 2020; Levit et al., 2018; Sóti et al., 2015; Vass et al., 2019a). Although the mentioned advantages make the technique suitable for pharmaceutical applications, there are still some key challenges that need to be addressed.

Besides increasing the dissolution of the potential drug molecules, the development of the technologies and integration of continuous manufacturing (CM) processes is a hot topic nowadays in the pharmaceutical industry too. The marketed products prepared by CM and the increasing number of publications about CM show that continuous technologies get more and more attention in the pharmaceutical field (Burcham et al., 2018; Lawrence and Kopcha, 2017). Nonetheless, there are two FDA-approved CM medicines contain spray-dried samples, which indicate the opportunities in the simultaneous application of ASDs and CM (Szabó et al., 2019). Although spray drying is a widely used method with high productivity, only a few publications have been published relating to the CM of spray-dried materials to tablets (Adali et al., 2020; Hu et al., 2011; Vanhoorne et al., 2016). From the industry point of view, the two FDA-approved spray-dried material-loaded CM medicines confirm that the topic has great industrial relevance. Using CM in the case of other ASDs products might also be effective with respect to the practical application since a high volume of ASD-loaded products are manufactured year by year and the cost of production or the energy consumption can be reduced in this way (Burcham et al., 2018; Pandi et al., 2020). However, it is worth keeping in mind that the handling of products with poor flowability is a general challenge for tablet development and it is even more difficult during the CM of spray-dried samples or electrospun materials with low bulk densities (Al-Zoubi et al., 2021). Therefore, overcoming the flowability problems of critical materials such as active pharmaceutical ingredients (APIs)

or ASDs is a crucial part of continuous process development (Besenhard et al., 2016; Chattoraj and Sun, 2018; Pingali et al., 2009; Szabó et al., 2019).

In general, one of the most critical parts of continuous tablet preparation is the feeding because it has a great influence on the homogeneity and the content uniformity of the blend and later the tablets (Blackshields and Crean, 2018). Consequently, the feedability of materials with poor flow properties needs to be improved with different formulation techniques. In the case of APIs or poorly flowable excipients, the most common method is coating the given material with silica, which improves the flowability and thereby the performance of the feeding (Escotet-Espinoza et al., 2020; Kunnath et al., 2018; Mullarney et al., 2011). Besides, the feedability enhancement can also be done through equipment design, for instance via application of vibratory feeders since the danger of clogging, and electrostatic charging of the particles is less than in the case of the twin-screw feeders (Besenhard et al., 2016). However, not only accurate feeding but also effective blending is important to prepare appropriate tablets continuously. The homogeneity of the blend largely depends on the process parameters of the continuous blending thus the determination of the influencing factors is a significant element of the process development (Liu et al., 2018; Vanarase et al., 2013).

Furthermore, introducing the process analytical technology (PAT) principles, the drug content needs to be monitored during the continuous blending to produce good quality products. Besides, the use of in-line analytical methods may contribute to the feedback control of the processes, which is a critical part of CM systems (Nagy et al., 2017). To accomplish quick, real-time determination of the API content, different non-destructive in-line analytical tools must be applied (De Beer et al., 2011). A widely used method is the near-infrared (NIR) spectroscopy, which has been already used successfully in many continuous blending processes (Colón et al., 2014; Koller et al., 2011; Vanarase et al., 2010). Similar results can be achieved by Raman spectroscopy since the organic API molecules have strong signals in the Raman spectrum (Nagy et al., 2019; Vergote et al., 2004). The real-time monitoring of the homogeneity and drug content has an important role in the process development because the effect of different parameters can be followed continuously (Martínez et al., 2013).

CM of electrospun material containing tablets is a rarely researched area because the industrial relevant scaled-up production of API-loaded fibers has not yet spread. The commonly used single needle electrospinning apparatus has very low productivity, circa 0.01-1 g/h (Vass et al., 2019c); therefore, it of limited use for ASDs where production rates of double digit kg/h are typically required (Jermain et al., 2018; Pandi et al., 2020). To achieve

the necessary production rate, different electrospinning principles and equipment designs have been researched to increase the efficiency of the technology (Vass et al., 2019c). For instance, the multi-jet electrospinning utilizes more needles (Kumar et al., 2010), the free surface electrospinning methods are based on the curvature formation of the solution surface (Ahmed et al., 2020; Jiang and Qin, 2014), the alternating current electrospinning replaces the common used direct current techniques (Farkas et al., 2019; Kessick et al., 2004), and high speed electrospinning (HSES) takes the advantage of both electrostatic forces and centrifugal forces (Nagy et al., 2015). The latter can be very promising from the pharmaceutical application point of view since even a 450 g/h production rate is achievable and the technology is considered scale-able (Nagy et al., 2015) and is similar to rotary spray dryers, which are scale-able to large capacity (Masters, 1985).

The second main question relates to the conversion of the electrospun fibers into a final dosage form. Although preparing orally dissolving webs via electrospinning is an easy and possible solution for pharmaceutical usage (Balogh et al., 2018; Celebioglu and Uyar, 2019; Sipos et al., 2019), the manufacture of the most commonly used dosage forms of capsules and tablets using electrospun fibers is more complicated due to their physical properties such as low bulk density or the fibrous structure (Démuth et al., 2017). The tableting of the pure electrospun products seemed to be possible in lab-scale (Hamori et al., 2016) but an industrially relevant process requires the application of the appropriate downstream steps and the suitable excipients (Démuth et al., 2016; Vass et al., 2019b). Besides, coupling continuous processing steps to the electrospinning is also challenging since the electrospun products with low bulk density can cause difficulties during the feeding, blending and tableting (Szabó et al., 2018). Increasing the flow properties of fluffy fibers via milling is the key point for preparing tablets (Vass et al., 2019b).

The main goals of the current research were to investigate the continuous downstream processing of milled electrospun fibers to tablet form for the first time and to develop in-line analytical methods for determining the ASD content, and thus the API content in real-time. An integrated system consisting of continuous feeding, blending and tableting was tested for the continuous manufacture of electrospun materials. Furthermore, the comparison of two non-destructive, in-line analytical tools, namely NIR and Raman spectroscopy, was also performed to investigate their applicability during continuous downstream processing of electrospun samples. The development of a fully continuous manufacturing line using electrospinning coupled with the appropriate PAT tools might be very promising in the pharmaceutical industry for effective manufacture of ASDs.

2. Materials and methods

2.1. Materials

Itraconazole (ITR) and vinylpyrrolidone-vinyl acetate 6:4 copolymer (PVPVA64) were obtained from Janssen Pharmaceutica (Beerse, Belgium). Microcrystalline cellulose (Vivapur® 200) and sodium stearyl fumarate (Pruv®) were received from JRS Pharma (Rosenberg, Germany). Mannitol (Pearlitol® 400DC) was a kind gift from Roquette Pharma (Lestrem, France). Crosslinked polyvinylpyrrolidone (Kollidon® CL) was given by BASF (Ludwigshafen, Germany). Aerosil® 200 was supplied from Evonik Industries (Essen, Germany). Reagent grade dichloromethane and ethanol were purchased from Merck Ltd. (Budapest, Hungary).

2.2. High speed electrospinning (HSES)

Electrospinning of the ITR-loaded fibers was accomplished using HSES equipment, which was combined with a cyclone (Figure 1) (Vass et al., 2019a). A fan provided a constant 120 m^3/h gas flow rate in the system during the whole production period. The key element of the apparatus is the stainless steel, round-shaped spinneret with 36 orifices (d = 500 μm) on its edge. This spinneret is connected to a pneumatic air-bearing turbine to reach a high rotation speed. The rotation speed of the spinneret was set to 40000 rpm. The preparation of fibrous product was carried out at 25 °C ± 1°C and 45 ± 5% relative humidity, while the applied voltage was fixed at 40 kV. The solid material concentration of the investigated composition was 0.375 g/ml (consisted of 40% ITR and 60% PVPVA64) and the solids were dissolved in the mixture of dichloromethane:ethanol (volume ratio 2:1) (Nagy et al., 2015). The solution containing the drug and the polymer was fed with a built-in peristaltic pump (Watson−Marlow Fluid Technology Group, Budapest, Hungary) with a flow rate of 1000 mL/h.

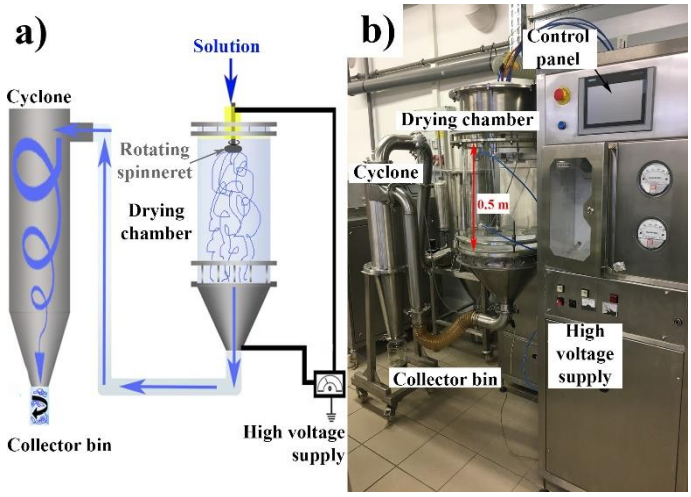

Fig. 1. Schematic drawing (a) and photo (b) of the applied high speed electrospinning (HSES) apparatus connected with a cyclone.

2.3. Milling of the electrospun product

A QUICKmill Lab multifunctional milling apparatus (Quick2000 Ltd., Tiszavasvári, Hungary) was used to reduce the fiber length to increase the bulk density and thereby to obtain a powder from the fibrous material with better flow properties (Section 3.1.). The equipment can be operated both in oscillating and conical milling mode depending on the applied grinding head. During this work, the oscillating mode was chosen due to its higher capacity and less material loss. A sieve with holes of 2.0 mm was used for the milling of the prepared electrospun sample. The milling rate was adjusted to 200 cycle/min, which resulted in circa 200 g/h milling capacity in the case of the investigated ITR-loaded fibrous system.

2.4. Characterization of the electrospun product

The basic characterization of the ITR-loaded electrospun material after milling was performed using differential scanning calorimetry, X-ray powder diffraction, in vitro dissolution testing, scanning electron microscopy, and laser diffraction measurements, as in our previous studies (Démuth et al., 2017; Démuth et al., 2018; Nagy et al., 2015). Non-milled fibers were investigated only by scanning electron microscopy since the non-milled samples cannot be examined by laser diffraction and the results of all the other measurements did not show any differences between the milled and non-milled samples according to prior experiences. Besides, the amount of the residual solvents is also a crucial factor during the application of solvent-based methods, which can examine well with headspace gas chromatography (Balogh et al., 2018). The method in the case of ITR-loaded fibers was similar than in one of our prior studies (Nagy et al., 2012). Our previous researches connected to the same composition showed that 700 ppm of ethanol and 300 ppm of dichloromethane

was found in the ITR-loaded electrospun samples after two days of storage at normal circumstances (open air), which values were far under the regulation limits (5000 ppm and 600 ppm for ethanol and dichloromethane, respectively). During this work, the electrospun fibers were used in further experiments only few days later thus residual solvents determination was not performed.

The prepared sample proved to be amorphous (Figure S1 and S2) and showed good dissolution (Figure S3). Since the basic characterization of the same composition was detailed in our previous studies, only the results of the newest in vitro dissolution tests, the scanning electron microscopy records, the particle size analysis and the bulk-tapped density test are showed in this paper. Therefore, only the above-mentioned methods are detailed in the following subsections.

2.4.1. In vitro dissolution tests

In vitro dissolution studies were carried out on a Pharmatest PTWS 600 dissolution tester (Pharma Test Apparatebau AG, Hainburg, Germany). The pure electrospun samples and the reference crystalline API were examined by the combination of the USP I and USP II method (tapped-basket method) (Nagy et al., 2015). The fibrous materials were milled and then the powders were weighted into the dissolution baskets. The dissolution of tablets was measured with the common USP II (paddle) method. The drug content was 50 mg in each case. The applied dissolution media was 900 mL of 0.1 N HCl set at a constant temperature of (37 ± 0.5) °C. The stirrer speed by the tapped-basket method and by the paddle method were 50 and 100 rpm, respectively. An Agilent 8453 UV–Vis spectrophotometer (Hewlett-Packard, Palo Alto, USA) was connected to the dissolution tester through flow cells to on-line measure the concentration of the dissolved ITR. Based on a preliminarily built calibration at a wavelength of 254 nm (from 1 to 50 mg/L), the concentration of the dissolved ITR was calculated in real-time during the measurements. Each different sample was investigated in triplicate.

2.4.2. Scanning electron microscopy

A JEOL JSM 6380LA (JEOL, Tokyo, Japan) type scanning electron microscope (SEM) was utilized for examining the morphology and size of the ITR-loaded electrospun material. The investigated specimen was fixed with conductive double-sided carbon adhesive tape. To avoid electrostatic charging, the electrospun sample was sputtered with gold in the next step of sample preparation. The SEM measurement was accomplished in a high vacuum. The applied working distance was 15 mm while the accelerating voltage was 15 kV.

Calculation of the average fiber diameter was performed by a randomized diameter determination method (Balogh et al., 2015).

2.4.3. Particle size analysis

The particle size distribution of the electrospun sample after milling was determined by a Malvern Mastersizer 2000 type laser diffractometer (Malvern Instruments Ltd., Worchestershire, UK). Before the measurement, a background recording was adjusted for 45 seconds. Then a vibratory feeder added the powder into the equipment with 75% intensity of the vibrational amplitude. The measurement took 60 seconds while the applied pressure was 1.5 bar. The measured $d_{(0.5)}$ values were described as the 50% cumulative undersize of the volumetric distribution, which was used to characterize the particle size.

2.4.4. Bulk and tapped density test

Furthermore, the bulk and tapped densities of the milled electrospun material were also investigated using an ERWEKA SVM12 (Heusenstamm, Germany) type tapped density tester. The flow property of the powder was determined based on the calculated Hausner ratio and the Carr index (Carr, 1965; Hausner, 1967).

2.5. Continuous blending and tableting

The targeted API content was 50 mg per 600 mg tablet, which was equal to 125 mg 40% ITR-loaded electrospun material (Démuth et al., 2017). The experimental set-up of continuous blending and tableting consisted of two feeders, a twin-screw blender, a conveyor belt and a tableting machine (Figure 2).

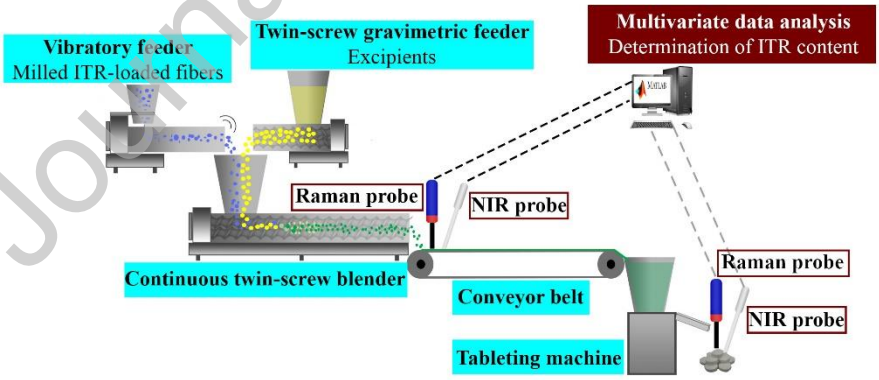

Fig. 2. Schematic illustration of the continuous experimental set-up.

The milled ITR-loaded fibers were fed into the blender with a LABORETTE 24 vibratory feeder (Fritsch GmbH, Idar-Oberstein, Germany). During the experiments, a V-shaped channel was applied to direct the powder into the blender. The feeding rate could be controlled by adjusting the vibration amplitude. Since gravimetric feeding could not be

performed with this feeder, a pre-calibration of the vibration amplitude and the feeding rate was accomplished before each experiment to set the feeding rate to the targeted API content. The pre-blend of all other excipients (including the lubricant) was fed with a Brabender DDW-MD0-MT type (Brabender Technologie, Duisburg, Germany) twin-screw feeder in gravimetric mode. The adjusted feeding rate was 750 g/h to achieve appropriate API content in the blend.

A TS16 QuickExtruder® (Quick 2000 Ltd., Tiszavasvári, Hungary) multifunctional equipment was applied for continuous twin-screw blending. The diameter of the screws was 16 mm, while the L/D ratio was 25. The rotation speed of the screws was set to 70 rpm during the continuous blending of the electrospun sample and the excipients.

After the continuous blending, a conveyor belt carried the existing powder mixture from the blender to the tableting machine. The tablets were compressed on a Dott Bonapace CPR6 eccentric tableting machine (Limbiate, Italy) using 14 mm round-shaped punches. The 600 mg tablets were prepared with about 10 kN compression force. The upper and lower punches were set before the continuous experiment.

The continuous line set-up was supplemented with NIR and Raman probe in reflection mode to collect real-time spectra of the ITR-loaded powder mixture. Both spectroscopic techniques were suitable to obtain spectra of tablets thus off-line investigations after the tableting process was accomplished as well. The spectrum accumulation was achieved using the OPUS 7.5 (Bruker Optik GmbH, Germany) and iC Raman® (Mettler-Toledo AutChem Inc.) softwares during the NIR and Raman spectroscopic analyses, respectively. Besides, MATLAB 9.4.0. (MathWorks, USA) and PLS Toolbox 8.6.1. (Eigenvector Research, USA) were applied for real-time evaluation of the measured spectra. Two Matlab scripts have been developed in-house to get real-time information about the ASD concentration of the blend based on the calibration with the electrospun material-loaded powders (Gyürkés et al., 2020; Nagy et al., 2017). The first script is aimed to continuously import the acquired spectra into Matlab during the experiments, while the second script dealt with the chemometric analysis of the spectra using the PLS model built in PLS Toolbox. The second script continuously recorded the ASD concentration calculated from the chemometric analysis thus the current ITR-loaded electrospun material content could be monitored in real-time during the whole continuous blending experiment.

2.6. NIR spectroscopy

A Bruker MPA Multi Purpose Fourier-transformed Near Infrared (FT-NIR) Analyzer (Bruker OPTIK GmbH, Germany) with a high intensity NIR source (Tungsten) and PbS

detector was utilized as one of the PAT tools for monitoring the continuous blending and investigation of the prepared tablets. The spectra were collect in reflection mode while the investigated spectral range was set to 4000-10000 cm^{-1}. The resolution of 8 cm^{-1} was applied during the measurements and 16 scans were accumulated with double-sided, forward-backward acquisition mode. 5 spectra per blend and 6 measurements per 3 tablets (both sides of each tablet) were used for calibration.

2.7. Raman spectroscopy

A Kaiser RamanRxn2® Hybrid in situ analyzer (Kaiser Optical Systems, Ann Arbor, USA) equipped with PhAT (Pharmaceutical Area Testing) probe was used for in-line detection of the ASD content after the continuous blending. A 400 mW, 785 nm diode laser (Invictus) was applied for illuminating the samples. The diameter of the laser spot size was adjusted to 6 mm and the nominal focal length was 250 mm. The 200-1890 cm^{-1} spectral range was investigated with 4 cm^{-1} resolution and 1690 variables were collected during the data processing. Reflection mode was utilized for measuring the calibration samples (blends and tablets) and for monitoring the continuous blending process. The tablets prepared after the continuous blending were investigated in reflection mode as well. The number of repetitions for calibration was the same as in the NIR experiments. The applied acquisition time was 5 seconds with two scans during the calibration and measuring of blends and tablets.

2.8. Multivariate data analysis

Each calibration sample consisted of the mixture of the excipients and the electrospun sample in different concentrations. The composition of the excipients-loaded powder was chosen based on a prior study and it is summarized in Table 1 (Démuth et al., 2017). To develop a suitable chemometric model for the target concentration (20.8 w/w% electrospun material), the ASD contents of the calibration samples were 0, 5, 10, 15, 20, 20.8, 25 and 30 w/w%, which are equal to 0, 2, 4, 6, 8, 8.3, 10 and 12 w/w% API content. Besides, 7, 13 and 22 w/w% ASD-loaded samples were also prepared for validation of the blend models. The homogenization of the calibration blend was performed with the previously mentioned QUICKmill Lab multifunctional milling apparatus, where the grinding head was changed to a batch bin blender. The powder mixtures were homogenized for 5 minutes with a rotation speed of 60 rpm. The tablets for calibration were pressed from the prepared calibration blends.

Table 1

Composition of the excipients powder mixture and the target blend. (ITR abbreviation indicates the itraconazole while the PVPV64 acronyms refers to the vinylpyrrolidone-vinyl acetate 6:4 copolymer.)

Material (function)	Concentrations in the blend of excipients (w/w%)	Concentrations in the target composition (w/w%)
Pearlitol®400DC (filler)	42.1	33.35
Vivapur®200 (filler)	42.1	33.35
Kollidon®CL (disintegrant)	12.6	10
Aerosil® (glidant)	1.3	1
Pruv® (lubricant)	1.9	1.5
Electrospun sample (40% ITR + 60% PVPVA64)	-	20.8

The evaluation was accomplished by using MATLAB 9.4.0. (MathWorks, USA) program with PLS Toolbox 8.6.1. (Eigenvector Research, USA). During the evaluation process, a calibration curve was determined with the partial least squares (PLS) regression method, using the ASD content as dependent variable. Important to note that the milled electrospun fibers containing both ITR and PVPVA64 were used in the calibration samples thus in the calibration spectra, the spectral signs of the prepared ASD were characteristics and not of the pure API. Therefore, the calibration models were built on the ASD content and not on the API content. However, the API content of the electrospun fibers was also determined by UV-Vis measurements before the calibration. The number of latent variables was chosen by minimizing the root mean square error of cross-validation ($RMSE_{CV}$). Interval PLS method proved to be suitable in all cases for variable selection, where the number of maximal latent variables was changed based on the pretreated PLS model. All of the NIR spectra were pre-processed using Savitzky–Golay first derivative (a second-order polynomic function was fitted, while the number of points in the filter was fifteen, and only included data were applied). Multiplicative signal correction (MSC) using the mean spectra as reference and mean centering were also applied in the further steps of NIR spectra pretreatment. The Raman spectra were smoothed at first with Savitzky–Golay smoothing method (a second-order polynomic function was used, while the number of points in the windows was fifteen, and only included data were applied). Then all Raman spectra were baseline corrected using Automatic Whittaker Filter baseline correction with an asymmetry parameter $p = 0.001$ and a smoothing parameter $\lambda = 10^5$. The Raman spectra of the blends were normalized to unit length, which is a widely used weighted normalization method. The intensity of the raw spectra showed greater differences (see Figure S5) thus this form of normalization, where the larger values were weighted more heavily in the scaling, seemed to be suitable for the spectra

of calibration powders. The intensity values of the Raman spectra of the different concentration tablets were closer to each other; therefore, these raw spectra were normalized to unit area, which proved to be appropriate for these data (Figure S5). In the final step of the pre-processing, mean centering was utilized in the case of the Raman spectra as well. For cross-validation, 6-fold and 7-fold venetian blind cross-validation were used, leaving out one sample per concentration levels at each calculation step methods , in the case of the blends and tablets, respectively. This validation found to be suitable since the replicate measurements were ordered randomly. Besides, external validation was also performed in the case of powders, which confirmed the applicability of the built models.

The models were compared by the coefficient of determination for calibration, cross-validation, and prediction (R^2_C, $R^2_{CV,}$ R^2_P), and the root mean square error of calibration, cross-validation, and prediction ($RMSE_C$, $RMSE_{CV}$, $RMSE_P$). The performance of the built models was also characterized by the limit of detection (LoD) and limit of quantification (LoQ), which were calculated by equations 1 and 2 (de Carvalho Rocha et al., 2012). Furthermore, the limit of Hotelling T^2 was calculated in the case of the selected models to determine an acceptance limit for the real-time experiment (equation 3) (Nagy et al., 2017).

$$\mathrm{LoD} = \frac{3.3 \times \sigma}{S} \quad (1)$$

$$\mathrm{LoQ} = \frac{10 \times \sigma}{S} \quad (2)$$

$$\text{Limit of Hotelling } T^2 = \sigma_{\text{Hotelling } T^2} + (3 \times \text{Hotelling } T^2{}_{\mathrm{MAX}}) \quad (3)$$

In equations 1-2, σ indicates the standard deviation (SD) of the predicted y-values for each x-value; S denotes the slope calculated from the measured and predicted concentrations. The calculation of these values are detailed in the supplementary materials (Eq. S1 and S2). In equation 3, $\sigma_{\mathrm{HotellingT}^2}$ means the standard deviation of the Hotelling T^2 values and Hotelling $T^2{}_{MAX}$ expresses the largest Hotelling T^2 value of the given model.

2.9. Determination of content uniformity

The content uniformity in the tablets was measured with UV-Vis spectroscopy, which was applied as a reference analytical method for verifying the results of the NIR and Raman spectroscopy measurements. The same wavelength and calibration were used as for the *in vitro* dissolution tests to determine the ITR concentrations in the tablets. The tablets were dissolved in 2 L of 0.1 N HCl dissolution media and stirred with a magnetic stirrer for 2 days. The solutions were filtered through a 0.45 μm filter before the UV-Vis measurements.

2.10. Characterization of tablets

Friability was measured on PharmaTest PTF 20E (Hainburg, Germany) type friability tester after 100 rounds on 10 tablets. Tablet breaking force was determined on a Schleuniger 4 M (Thun, Switzerland) type hardness tester with 10 tablets. A Sartorius MA40 (Göttingen, Germany) moisture analyzer was used for measuring the moisture content of 10 ground tablets. Loss in drying was determined at 105°C for 10 minutes. The thickness of the tablets was determined with a Pro-Max Electronic Digital Caliper (NSK, Tokyo, Japan).

3. Results and discussion

3.1. Preparation of the electrospun and milled samples

The development of an integrated continuous formulation system requires the synchronization of each processing step with respect to capacity. During this research, the production rate of the electrospinning experiments was chosen to fit the next milling step, while the further steps (feedings, blending, tableting) were adapted to the production rate of the milled fibers to see the potential of a possible fully continuous line (from the electrospinning to the tableting). The feeding rate of the solution was set to 1000 mL/h, which seemed to be suitable to prepare adequate quality fibers (grindable, dry product with small fiber diameter). The yield of 78% was reached with the applied process parameters, which resulted in ~ 200 g/h production rate for the solid fibrous material. During longer productions, the yield of the electrospinning might be further enhanced. On the other hand, the material loss was observed on the wall of the drying chamber thus further optimization of the formulation and the equipment (e.g. additional air knives in the HSES equipment) could further increase the yield. The basic characterization showed similarities to the results of our previous articles (data not shown), which means that electrospun fibers containing an ASD of 40% ITR and 60% PVPVA64 with good dissolution properties (90% released within 10 min) were prepared using the aforementioned settings (Nagy et al., 2015).

Milling of the fibrous products may result macroscopically near round-shaped particles with enhanced flowability therefore, it is important to choose well grindable API-polymer compositions for electrospinning. The ITR-PVPVA64 system was easy to grind with an oscillating milling machine right after the ES because the powder did not stick into the hole of the sieve and the material loss was less than 5%. The successful milling right after the HSES assumes that the fibers dried enough during the continuous fiber collection by cyclone. The average diameter of the ITR-loaded electrospun fibers was 1.6 ± 0.9 µm and the fibrous structure remained after the oscillating milling (Figure 3).

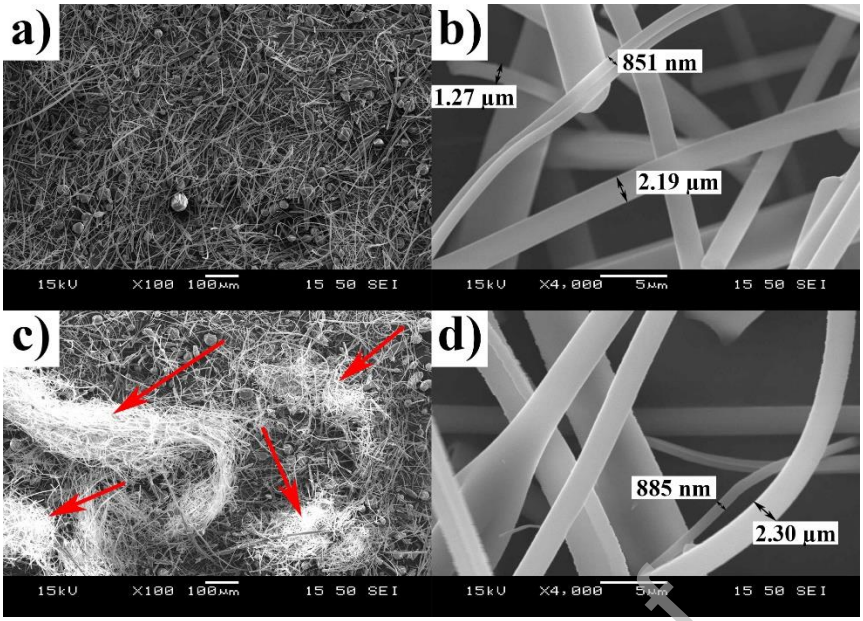

Fig. 3. Scanning electron microscopic images of the prepared electrospun sample a) before milling (100× magnification); b) before milling (4000× magnification); c) after milling (100× magnification) (red arrows indicate the entangled fibers); d) after milling (4000× magnification).

The macroscopic characteristic of the milled product was investigated with laser diffraction and the results are shown in Figure 4 and Table 2. The observed multimodal particle size distribution with an average diameter of 12.6 ± 1.0 µm can be explained by the formation of different sized agglomerates after the milling. The high standard deviations and relative standard deviations suggest inhomogeneity in the macroscopic particle size after the milling, which can be a critical factor during the downstream processing of the milled fibers. The SEM images also presented that the milled fibers became entangled and form smaller and larger agglomerates or bundles (Figure 2b).

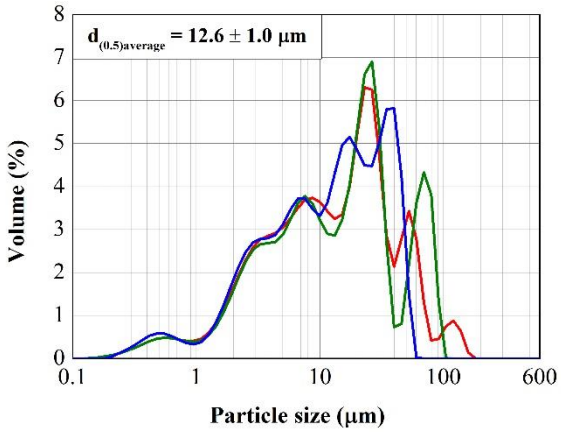

Fig. 4. The particle size distribution of the ground ES sample. Different colors indicate three repeated measurements from the same sample.

Table 2

Results of the laser diffraction measurements.

	$d_{(0.1)}$	$d_{(0.5)}$	$d_{(0.9)}$
Average (µm)	2.1	12.6	47.4
Standard deviation (µm)	0.1	1.0	11.6
Relative standard deviation (%)	3.5	8.2	24.5

Although the size distribution of these agglomerates showed higher deviations, the flowability of the milled fibers found to be good according to the bulk-tapped density test (Table 3) thus the sample seemed to be suitable for further downstream processing steps. However, the milled fibrous material still has a low bulk density (~ 0.13 g/cm^3) and is prone to electrostatic charge, which can cause difficulties during the formulation (e.g. the sample could stick to the wall of the feeder, blender, and tableting machine and lead to weight variations during the processes). For this reason, the application of excipients with good flow properties such as large particle size microcrystalline cellulose or mannitol (Démuth et al., 2017), and effective blending is indispensable to continuously produce tablets. Furthermore, the investigated electrospun system with low bulk density revealed that the applicability of the powders cannot be predicted based on only the Hausner ratio and Carr's index. Wider powder characterization can give more information about the materials with respect to the formulation processes (Van Snick et al., 2018).

Table 3

Results of the bulk-tapped density test. Standard deviations were calculated from three repeated measurements.

ρ_{bulk} (g/cm^3)	0.13 ± 0.01
ρ_{tapped} (g/cm^3)	0.15 ± 0.01
Hausner ratio	1.15 ± 0.02
Carr's index	13 ± 1.22

3.2. Preliminary experiments before PAT-based continuous blending and tableting

Before the continuous blending and tableting experiments in-line analytical methods needed to be developed to determine the drug content in real-time. Coupling of in-line applicable PAT tools to the CM processes can ensure good quality products. During the continuous formulation of electrospun samples, monitoring of the ASD content, and thus the API content (section 2.8.) is the key factor from the quality point of view. Preliminary experiments showed the applicability of NIR and Raman spectroscopies for the analysis of the ITR-loaded electrospun materials during continuous blending. However, the quantitative determination of the ASD content required thorough calibration and chemometric model building.

3.2.1. Effect of the lubricant

One of the crucial parts of the method development was the preparation of the calibration samples. The first important question, had to be considered, was how to add the lubricant. A possible answer is the feeding of the lubricant directly before the tableting since the over-lubrication can be avoided in this way. However, continuous feeding of the lubricants with poor flowability may be challenging, therefore a pre-blend with the other excipients was more suitable from the CM point of view. For this reason, the effect of the sodium-stearyl-fumarate (SSF) on the dissolution was investigated first to see if it could be added to the mixture of the excipients before the continuous blending with the electrospun material. To test the impact of the lubricant, tablets were prepared in small quantities with batch homogenization method. The results showed that the tablets, where the SSF was added to the powder mixture with the other excipients and electrospun sample and homogenized for 30 minutes showed similarities with the dissolution of the tablets, where the SSF was added only after the homogenization of the blend for 30 minutes (Figure 5). Although the applied homogenization times during the batch blending processes were much higher than the residence times during a CM, the dissolution did not deteriorate. Therefore, it can be stated that the lubricant does not mean a problem in the case of the examined composition and processing steps, thus the SSF was added to the calibration samples as well.

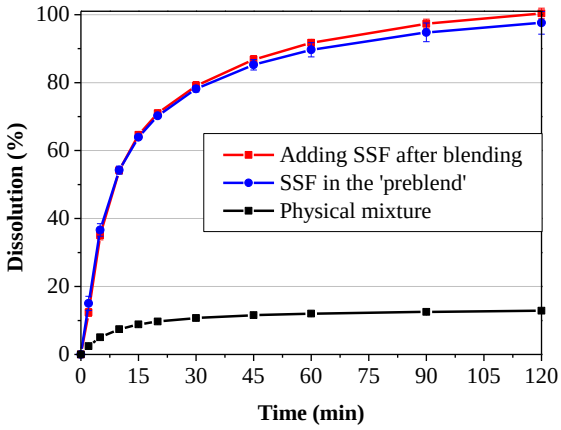

Fig. 5. Investigation of the effect of the lubricant on the dissolution of the ASD-loaded tablets (900 mL 0.1 M HCl dissolution medium, 37±0.5°C, 100 rpm, paddle method, 50 mg API content, n = 3). The physical mixture contained the crystalline ITR, the polymer and the tableting excipients in the same concentrations as the ASD-loaded tablets.

3.2.2. Chemometric model building

To reduce the time and the material consumption of the calibration, 2.4 g blends were prepared at each concentration and measured off-line mode without any special sample preparation and destruction. Then the NIR and Raman spectra were pre-processed to find the most reliable regression models. Several variable selection methods were also tried for choosing the appropriate spectral regions that carry the most information. The raw and the pre-processed NIR and Raman spectra of the powders can be seen in Figure S4 and S5, respectively. The off-line performance characteristics of the selected models seemed to be satisfying according to the R^2, RMSE and bias values (Table 4). Although the LoD and LoQ values proved to be lower for the NIR spectra-based model, the Raman spectroscopy also seemed to be appropriate to predict accurately the concentrations around the target value.

Table 4

Off-line performance parameters of the selected models.

	NIR spectra-based model	Raman spectra-based model
Number of latent variables	3	6
R^2_C	0.994	0.997
R^2_{CV}	0.988	0.990
$RMSE_C$ (w/w%)	0.727	0.502
$RMSE_{CV}$ (w/w%)	1.035	1.004
$Bias_C$ (w/w%)	0.000	0.000
$Bias_{CV}$ (w/w%)	-0.013	-0.081
LoD (w/w%)	2.47	4.93

LoQ (w/w%)	7.48	14.93

The main goal of this work was to develop in-line applicable models to the continuous blending thus off-line performance parameters of the models needed to be supplemented with other important indicators. Before the real in-line tests, the validation of the selected models was accomplished with 7, 13 and 22 w/w% ASD-loaded samples, which were made in the same way as the calibration samples but not used during the model building. The validation blends were measured five times and the concentrations were predicted by the selected models. The predicted values were subtracted from the known concentrations and the obtained residuals can be found in Figure 6. The residuals of the repeated measurements were below 5 w/w%, which indicates acceptable predicting performance. The higher SDs in the case of the 13% ASD-loaded sample can refer to the inhomogeneity of the validation sample and not the error of the models since the SDs of the other two investigated concentrations proved the be suitable. However, it can be stated that the Raman spectra-based model can predict the concentrations more accurately since the SDs of the repeated measurements were lower. Furthermore, the averaged results of the Raman-based model showed fewer deviations from the known concentration of the compositions; therefore, it could be more promising in the in-line applicability point of view than the NIR spectra-based model (Table 5). It is important to note that the calculated deviations agree with the LoD and LoQ values of the models since the highest differences were observed at the 7% ASD-loaded sample, which concentration is below the LoQ values of 7.48 and 14.93 in the case of NIR and Raman spectra-based models, respectively. Furthermore, the R^2_P and the $RMSE_P$ values were also calculated to see the goodness of the models (Table 5). These indicators suggest that the Raman spectra-based model can be more accurate to predict in-line the ASD content during a real-time continuous blending process. For outlier detection, the critical limit of Hotelling T^2 values was determined, which were 26.68 and 25.06 in the case of NIR and Raman spectra-based models, respectively. The Hotelling T^2 values of the validation samples were far under the calculated limits therefore both models seemed to be suitable for in-line application at these wider acceptance limits.

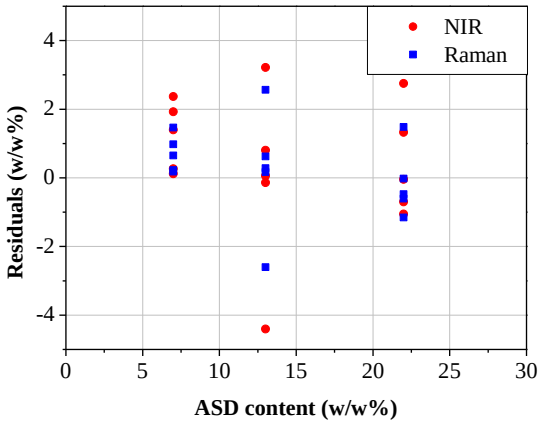

Fig. 6. Residuals of the validation samples in the function of ASD content (n=5).

Table 5

Prediction performance of the selected models.

			NIR spectra-based model	Raman spectra-based model
Prediction of the validation samples	7% ASD content	Average	8.21	7.70
		SD	1.00	0.54
		Percentage deviation (%)	17.34	9.98
	13% ASD content	Average	12.91	13.20
		SD	2.76	1.85
		Percentage deviation (%)	0.73	1.59
	22% ASD content	Average	22.45	21.84
		SD	1.57	1.00
		Percentage deviation (%)	2.06	0.71
R^2_P			0.917	0.964
$RMSE_P$ (w/w%)			1.874	1.199
$Bias_P$ (w/w%)			0.524	0.250

3.3. Continuous blending

3.3.1. Setting of the continuous blending experimental setup

NIR and Raman spectroscopies seemed to be appropriate to detect the ITR-loaded electrospun material in blends thus the next step was to investigate the in-line applicability of the built models during the continuous blending process. The continuous experiments required the application of suitable devices and setups, where the most critical processing step is the continuous feeding of the powders (Figure 7). The preliminary experiments revealed that the homogenization of the tableting excipients including the lubricant does not cause deteriorated dissolution therefore using a pre-blend during the continuous blending of

electrospun materials seemed to be a proper solution. The application of excipients composites provide several advantages and has industrial relevance as well since some powder mixtures for CM are already on the market (Pharma, 2016). In this way, fewer feeders need to be used for continuous blending processes, which decreases the possibility of weight variations due to feeding errors. The blend of the excipients was characterized with excellent flowability and 0.45 g/cm^3 bulk density thus it proved to be perfect for a CM process. Besides, the feedability of the powder was appropriate and well adjustable using a twin-screw gravimetric feeder. Although the feeding of the milled electrospun materials is more challenging due to the low bulk densities, a vibratory feeder was suitable for handling the prepared ITR-loaded fibers. A further crucial parameter was the rotation speed of the screws in the extruder during the continuous blending. On the one hand, if the rotational speed is too slow the accumulation of the electrospun sample in the extruder's hopper can stop the whole process. On the other hand, if the rotational speed is too fast the efficiency of the blending can decrease. For this reason, preliminary experiments were performed to find an optimal setting, where the rotation speed was changed from 50 rpm that found to be an appropriate setting to transport the mixture of excipients. The finally selected rotation speed was 70 rpm since this was the lowest adjustment, which proved to be suitable for efficient transport of the incoming pre-blend and electrospun fibers together. The bulk density of the outgoing blend was 0.43 g/cm^3 and its flowability proved to be appropriate for the tableting. At higher rotational speed, the powders were not able to totally fill the screws, which resulted in inhomogeneous blend.

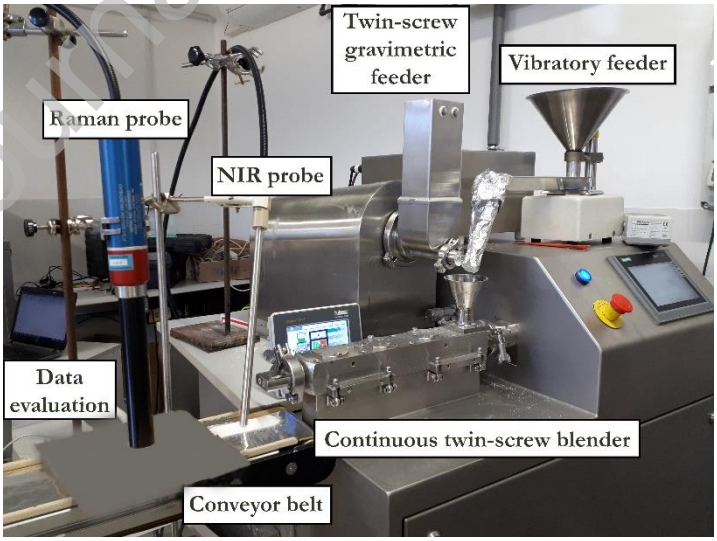

Fig. 7. Photo of the continuous blending experimental setup.

3.3.2. Real-time monitoring of continuous blending

To investigate the homogeneity of the outgoing blend in the case of the set rotation speed the developed NIR and Raman spectra-based models were applied in a continuous experiment (Figure 8). The aim of the continuous blending process was two-fold: to check the in-line applicability of the built PLS models, and to prepare homogenous electrospun ASD-loaded blend continuously, which was never accomplished before according to the best knowledge of the authors. At the beginning of the process, only the excipients were fed into the blender. Both the NIR and Raman spectra-based models calculated values around 0% but the NIR spectroscopy showed some outlier based on the Hotelling T^2 values, especially at the first few measured points. Since the powder layer on the conveyor belt was thinner when the excipients were fed, these outliers suggest that the NIR spectroscopy was more sensitive to the thickness of the powder flowing under the probe. For this reason, it is worth paying a special attention to the sample thickness and because of it to the appropriate selection of the screw speed during the continuous blending processes (Nagy et al., 2017). After the feeding of the electrospun material, the measured ASD content of the blend increased continuously, which was measured well with both applied spectroscopic methods. After emptying the vibratory feeder, the ASD content decreased to the starting point according to the NIR and Raman measurements, which also confirmed the efficiency of the built models.

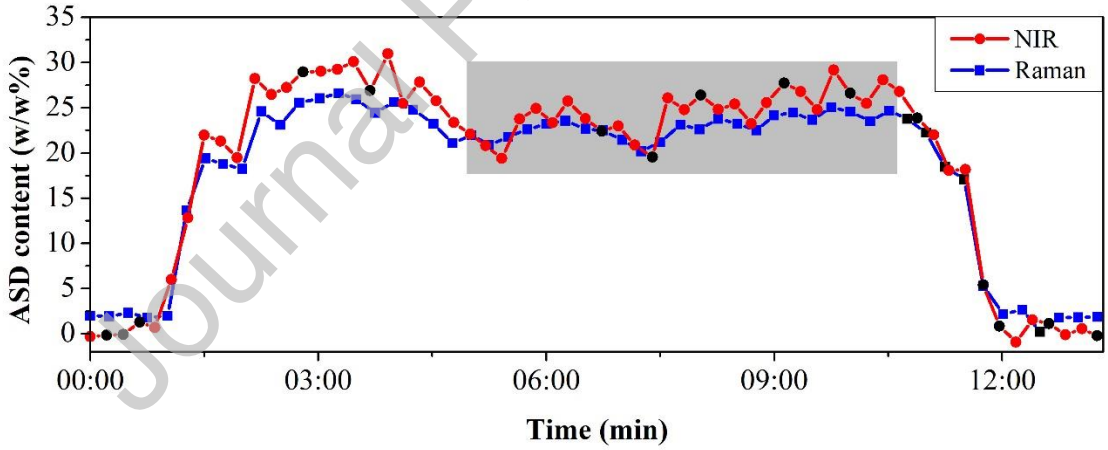

Fig. 8. Monitoring of continuous blending by NIR and Raman spectra-based chemometric models. Black symbols indicate the outliers from the models according to the calculated Hotelling T^2 limits. Grey background indicates that period when the feeding set up and the system reached a steady-state.

As expected based on the higher prediction performance values of the NIR validation, the NIR spectra-based model showed more outliers based on the Hotelling T^2 values, measured higher concentrations, and resulted in higher SD and relative standard deviation (RSD) in steady-state (Table 6). In contrast, the Raman monitoring showed more reliable

values and the ASD concentrations were closer to the target concentration (20.8 w/w%) during the steady-state. It is worth mentioning that the presented work is a proof-of-concept relating to the continuous manufacturing of electrospun fibers to tablet forms. Therefore, the variability was high from the industrial point of view but standard deviations can be decreased when fully integrated lines are constructed. To reach the target concentration more accurately, the feed-back control can be applied based on the Raman spectra (Nagy et al., 2017) or a gravimetric vibratory feeder could be used to adjust the feeding rate of the ASD.

Table 6

The averaged ASD and API content in steady-state.

		NIR spectra-based model	Raman spectra-based model
ASD content	Average	24.48	22.98
(w/w%)	SD	2.48	1.26
ITR content	Average	9.79	9.19
(w/w%)	SD	0.99	0.50
RSD		10.12	5.48

3.4. Characterization of continuously manufactured tablets

After reaching the steady-state, tablets were prepared and analyzed from the continuously blended powder (Figure 9). The obtained average hardness of ten examined tablets was 95 N while the loss in drying was 3.34% according to the moisture analysis. The thickness of the prepared tablets were between 4.38 and 4.42 mm. Besides, the friability was 0.67%, which is under the 1.00% regulatory limit determined for uncoated tablets. The measured values of the basic characterization methods met the usual pharmaceutical requirements and well correlated the previous results of the tablets containing ITR-loaded fibers (Démuth et al., 2017).

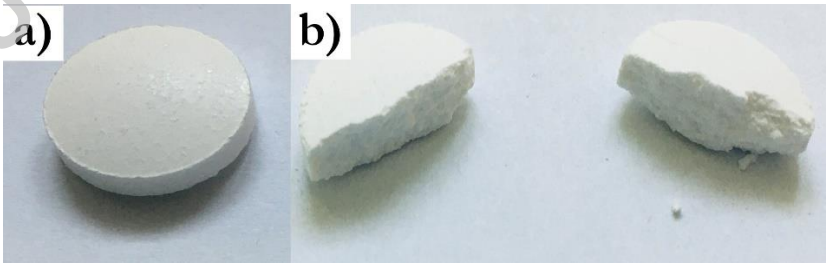

Fig. 9. Photos about a continuously prepared tablet (a) and a tablet after the hardness test (b)

For further investigations, ten tablets were selected randomly with an average tablet weight of 578.2 mg and measured off-line by NIR and Raman spectroscopy. The evaluation of the spectra was performed using the built models from the calibration tablets (Table 7). The

raw and the pre-processed NIR and Raman spectra of the tablets can be seen in Figure S4 and S5, respectively. The off-line performance parameters showed similarities to the models of the blends, and the LoD and LoQ values were also below the target concentration. The Hotelling T^2 values of the investigated tablets were well below the acceptance limit, as the highest values were 73.54 and 6.42 for the NIR and Raman measurements, respectively. Although the tablets were measured off-line, the low Hotelling T^2 values and the higher acceptance limits seemed to be promising thus it would be worth testing the models in-line.

Table 7

Off-line performance parameters of the selected tableting models.

	NIR spectra-based model	Raman spectra-based model
Number of latent variables	5	3
R^2_C	0.997	0.996
R^2_{CV}	0.988	0.993
$RMSE_C$ (w/w%)	0.541	0.620
$RMSE_{CV}$ (w/w%)	1.034	0.820
$Bias_C$ (w/w%)	0.000	0.000
$Bias_{CV}$ (w/w%)	0.088	0.021
LoD (w/w%)	3.99	2.09
LoQ (w/w%)	12.08	6.35
Hotelling T^2 limit	280.82	51.17

The API content of the selected tablets was measured by a reference UV-Vis method as well, and the calculated API content results from the three different measurements (NIR, Raman, UV-Vis) are depicted in Figure 10. The ITR content of each tablet was in a narrow range around the targeted 50 mg dose and the deviation of the average values from the target value was less than 5% in all cases (Table 8), which also proved the feasibility of the presented CM setup. The API concentration calculated by the three different measurements showed similarities, and the average ITR content of the ten tablets was comparable in all cases (Table 8).

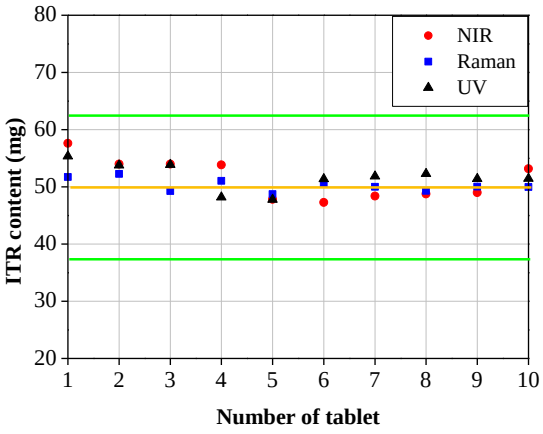

Fig. 10. ITR content of the randomly selected ten tablets in weight unit calculated from NIR, Raman and UV-Vis measurements. The yellow line indicates the target value and the green lines show the USP limit (Pharmacopeia, 2007.).

Table 8

Content uniformity test of the prepared ITR-loaded tablets. $\bar{X}$, s, M and AV numbers given as % label claim. M can be determined based on the sample mean. If 98.5 < $\bar{X}$ < 101.5 then M = $\bar{X}$, if $\bar{X}$ < 98.5 then M = 98.5, if X > 101.5 then M = 101.5. The AV = |M-$\bar{X}$ | + kS, where k = 2.4 for 10 tablets (Pharmacopeia, 2007.).

	NIR	Raman	UV
Average API content of ten tablets (mg)	51.4	50.3	51.7
SD (mg)	3.5	1.1	2.4
RSD	6.9	2.2	4.6
Deviation from the target value (%)	2.8	0.6	3.5
$\bar{X}$ (sample mean)	102.7	100.6	103.5
s (sample SD)	6.7	2.2	4.4
M	101.5	100.6	101.5
AV	17.3	5.3	12.6

The Acceptance Value (AV) of the tablets calculated by Raman and UV-Vis methods were below the L1 = 15.0 acceptance limit, which means that the tablets passed the USP <905> content uniformity test (Pharmacopeia, 2007.). Furthermore, the ITR contents of the individual tablets were between 37.5 and 62.5 mg, i.e. between 75.0 and 125.0% of the label claim (the 100.0% target content was 50 mg in this case). The NIR spectra-based model resulted in higher AV due to the higher RSD values but the predicted API contents were similar to the results of the other two methods. Besides, the NIR and Raman spectra-based models were compared according to the error of the prediction, where the UV-Vis results were used as known API content. The RMSEP values were 2.96 mg and 2.52 mg for the NIR and Raman spectra-based calculations, which proved to comply with the USP limits. The UV-

Vis measurements verified the reliability of the NIR and Raman methods, thus the traditionally used destructive and off-line UV-Vis analysis could be replaced with the in-line applicable, non-destructive NIR and Raman spectroscopy. The quality control can be simplified in this way, and it can be characterized as being time-efficient, since the spectra recording takes only a few seconds per tablet. Therefore, the API content of each tablet can be determined and a fully automated system is achievable, which enables even the implementation of real-time release tests (Markl et al., 2020).

Moreover, the shear forces during the blending process of electrospun materials are also crucial factors since a low-shear mixing may lead to unacceptable final homogeneity (Fülöp et al., 2018). The results of this work showed that there were no significant standard deviations in the content uniformity of the final dosage form, which suggests that the shear forces in the twin-screw blender were high enough to distribute the different size agglomerates of the milled fibrous material. Besides, volumetric feeding of the API-loaded fibers resulted in an appropriate content uniformity, but it could be further improved using a gravimetric vibratory feeder. Based on the results, CM of electrospun ASD-loaded tablets is achievable, and in-line spectroscopy-based feedback control of the feeders could further increase the efficiency of the processes.

4. Conclusions

Continuous manufacturing of tablets containing milled ITR-loaded electrospun fibers was successfully achieved through a multi-step system including electrospinning, milling, feeding, blending and tableting processing steps. The synchronization of the different parts of the investigated experimental setup was an important aspect of the work. The adjusted feeding rate during the electrospinning resulted in ~ 200 g/h ASD productivity and this value was the starting point of the continuous blending as well. For the examined ITR-PVPVA64 formulation, the results showed that it was possible to produce 600 mg tablets continuously. Further developments could enable a fully continuous line integrating electrospinning with milling to the continuous tableting process. In that case, the application of the presented production rates could result in circa 38.400 tablets/day in the case of the 600 mg tablets with 50 mg API content. Moreover, further scale-up is also achievable (Nagy et al., 2015), which can satisfy the requirements of the pharmaceutical industry.

Besides, real-time monitoring of the ASD content proved to be achievable using NIR and Raman spectroscopy and spectra-based PLS regression models. The off-line performance parameters of the models, the validation and the in-line experiments revealed that the Raman spectroscopy-based models are more robust and accurate than the NIR spectra-based models. The UV-Vis measurements, used as a reference analytical method, confirmed that appropriate homogeneity was achieved in the final dosage form, which was well measurable with both NIR and Raman spectroscopy with 2.96 mg and 2.52 mg $RMSE_P$ values, respectively. Furthermore, the prepared tablets fulfilled the USP <905> content uniformity test based on the results of UV-Vis and Raman spectroscopy. The implementation of the in-line, non-destructive methods in the continuous formulation of electrospun material allowed the determination of the ASD, and thus the API content in real-time, which reduced the time of the quality control from more than a day to 10 s per tablet. Furthermore, the feedback control of the excipients feeder based on the Raman spectra and the built chemometric model could make the whole continuous system more reliable. The simultaneous application of electrospinning and CM was demonstrated well in the present study and the combination of these two areas can open new ways in the development and production of effective solid dosage forms.

Credit Author Statement

- *Edina Szabó*

  Writing-original draft, investigation and writing-review and editing.
- *Petra Záhonyi*

  Investigation and writing-original draft
- *Martin Gyürkés*

  Investigation and writing-original draft
- *Brigitta Nagy*

  Resources and writing-review and editing
- *Dorián L. Galata*

  Investigation, visualization and writing-original draft
- *Lajos Madarász*

  Investigation and writing-original draft
- *Edit Hirsch*

  Visualization and writing-review
- *Attila Farkas*

  Resources and writing-review and editing
- *Sune K. Andersen*

  Supervision and writing-review and editing.
- *Tamás Vígh*

  Resources and writing-review and editing.
- *Geert Verreck*

  Resources and writing-review and editing
- *István Csontos*

  Supervision; writing-original draft; and writing-review and editing
- *György Marosi*

  Conceptualization; funding acquisition; validation; and writing-review and editing.
- *Zsombor K. Nagy*

  Conceptualization; funding acquisition; supervision; writing-original draft; and writing-review and editing.

Acknowledgement

This work was performed in the frame of FIEK_16-1-2016-0007 project, implemented with the support provided from the National Research, Development and Innovation Fund of Hungary, financed under the FIEK_16 funding scheme. This research was supported from grants by National Research, Development and Innovation Office of Hungary (grant numbers: KH-112644, FK-132133, PD-121143). Attila Farkas acknowledges the financial support received through the PREMIUM post-doctorate research program of the Hungarian Academy of Sciences. This project was supported by the ÚNKP-20-2-I and the ÚNKP-20-3-I New National Excellence Program of the Ministry of Human Capacities.

Declaration of interest

The authors report no conflict of interest.

References

Adali, M.B., Barresi, A.A., Boccardo, G., Pisano, R., 2020. Spray freeze-drying as a solution to continuous manufacturing of pharmaceutical products in bulk. Processes 8, 709.

Ahmed, A., Yin, J., Xu, L., Khan, F., 2020. High-throughput free surface electrospinning using solution reservoirs with different radii and its preparation mechanism study. J. Mater. Res. Technol. 9, 9059-9072.

Al-Zoubi, N., Gharaibeh, S., Aljaberi, A., Nikolakakis, I., 2021. Spray Drying for Direct Compression of Pharmaceuticals. Processes 9, 267.

Balogh, A., Domokos, A., Farkas, B., Farkas, A., Rapi, Z., Kiss, D., Nyiri, Z., Eke, Z., Szarka, G., Örkényi, R., Mátravölgyi, B., Faigl, F., Marosi, G., Nagy, Z.K., 2018. Continuous end-to-end production of solid drug dosage forms: Coupling flow synthesis and formulation by electrospinning. Chem. Eng. J. 350, 290-299.

Balogh, A., Farkas, B., Faragó, K., Farkas, A., Wagner, I., Verreck, G., Nagy, Z.K., Marosi, G., 2015. Melt-blown and electrospun drug-loaded polymer fiber mats for dissolution enhancement: a comparative study. J. Pharm. Sci. 104, 1767-1776.

Besenhard, M., Karkala, S., Faulhammer, E., Fathollahi, S., Ramachandran, R., Khinast, J., 2016. Continuous feeding of low-dose APIs via periodic micro dosing. Int. J. Pharm. 509, 123-134.

Blackshields, C.A., Crean, A.M., 2018. Continuous powder feeding for pharmaceutical solid dosage form manufacture: a short review. Pharm. Dev. Technol. 23, 554-560.

Burcham, C.L., Florence, A.J., Johnson, M.D., 2018. Continuous manufacturing in pharmaceutical process development and manufacturing. Annu. Rev. Chem. Biomol. Eng. 9, 253-281.

Carr, R.L., 1965. Evaluating flow properties of solids. Chem. Eng. 18, 163-168.

Celebioglu, A., Uyar, T., 2019. Fast dissolving oral drug delivery system based on electrospun nanofibrous webs of cyclodextrin/ibuprofen inclusion complex nanofibers. Mol. Pharm. 16, 4387-4398.

Chattoraj, S., Sun, C.C., 2018. Crystal and particle engineering strategies for improving powder compression and flow properties to enable continuous tablet manufacturing by direct compression. Journal of pharmaceutical sciences 107, 968-974.

Colón, Y.M., Florian, M.A., Acevedo, D., Méndez, R., Romañach, R.J., 2014. Near infrared method development for a continuous manufacturing blending process. J. Pharm. Innov. 9, 291-301.

De Beer, T., Burggraeve, A., Fonteyne, M., Saerens, L., Remon, J.P., Vervaet, C., 2011. Near infrared and Raman spectroscopy for the in-process monitoring of pharmaceutical production processes. Int. J. Pharm. 417, 32-47.

de Carvalho Rocha, W.F., Nogueira, R., Vaz, B.G., 2012. Validation of model of multivariate calibration: an application to the determination of biodiesel blend levels in diesel by near- infrared spectroscopy. J. Chemom. 26, 456-461.

Démuth, B., Farkas, A., Balogh, A., Bartosiewicz, K., Kállai-Szabó, B., Bertels, J., Vigh, T., Mensch, J., Verreck, G., Van Assche, I., Marosi, G., Nagy, Z.K., 2016. Lubricant-induced crystallization of itraconazole from tablets made of electrospun amorphous solid dispersion. J. Pharm. Sci. 105, 2982-2988.

Démuth, B., Farkas, A., Szabó, B., Balogh, A., Nagy, B., Vágó, E., Vigh, T., Tinke, A., Kazsu, Z., Demeter, Á., Bertels, J., Mensch, J., Van Dijck, A., Verreck, G., Van Assche, I., Marosi, G., Nagy, Z.K., 2017. Development and tableting of directly compressible powder from electrospun nanofibrous amorphous solid dispersion. Adv. Powder Technol. 28, 1554-1563.

Démuth, B., Galata, D., Balogh, A., Szabó, E., Nagy, B., Farkas, A., Hirsch, E., Pataki, H., Vigh, T., Mensch, J., Verreck, G., Nagy, Z., Marosi, G., 2018. Application of hydroxypropyl methylcellulose as a protective agent against magnesium stearate induced crystallization of amorphous itraconazole. Eur. J. Pharm. Sci. 121, 301-308.

Démuth, B., Galata, D., Szabó, E., Nagy, B., Farkas, A., Balogh, A., Hirsch, E., Pataki, H., Rapi, Z., Bezúr, L., 2017. Investigation of deteriorated dissolution of amorphous itraconazole: Description of incompatibility with magnesium stearate and possible solutions. Molecular pharmaceutics 14, 3927-3934.

Drosou, C.G., Krokida, M.K., Biliaderis, C.G., 2017. Encapsulation of bioactive compounds through electrospinning/electrospraying and spray drying: A comparative assessment of food-related applications. Dry. Technol. 35, 139-162.

Escotet-Espinoza, M.S., Scicolone, J.V., Moghtadernejad, S., Sanchez, E., Cappuyns, P., Van Assche, I., Di Pretoro, G., Ierapetritou, M., Muzzio, F.J., 2020. Improving feedability of highly adhesive active pharmaceutical ingredients by silication. J. Pharm. Innov.

Farkas, B., Balogh, A., Cselkó, R., Molnár, K., Farkas, A., Borbás, E., Marosi, G., Nagy, Z.K., 2019. Corona alternating current electrospinning: A combined approach for increasing the productivity of electrospinning. Int. J. Pharm. 561, 219-227.

Fülöp, G., Balogh, A., Farkas, B., Farkas, A., Szabó, B., Démuth, B., Borbás, E., Nagy, Z.K., Marosi, G., 2018. Homogenization of amorphous solid dispersions prepared by electrospinning in low-dose tablet formulation. Pharmaceutics 10, 114.

Gyürkés, M., Madarász, L., Köte, Á., Domokos, A., Mészáros, D., Beke, Á.K., Nagy, B., Marosi, G., Pataki, H., Nagy, Z.K., 2020. Process Design of Continuous Powder Blending Using Residence Time Distribution and Feeding Models. Pharmaceutics 12, 1119.

Hamori, M., Nagano, K., Kakimoto, S., Naruhashi, K., Kiriyama, A., Nishimura, A., Shibata, N., 2016. Preparation and pharmaceutical evaluation of acetaminophen nano-fiber tablets: Application of a solvent-based electrospinning method for tableting. Biomed. Pharmacother. 78, 14-22.

Hausner, H.H., 1967. Friction conditions in a mass of metal powder. Polytechnic Inst. of Brooklyn. Univ. of California, Los Angeles.

Hu, J., Ng, W.K., Dong, Y., Shen, S., Tan, R.B., 2011. Continuous and scalable process for water-redispersible nanoformulation of poorly aqueous soluble APIs by antisolvent precipitation and spray-drying. International journal of pharmaceutics 404, 198-204.

Jermain, S.V., Brough, C., Williams III, R.O., 2018. Amorphous solid dispersions and nanocrystal technologies for poorly water-soluble drug delivery–An update. Int. J. Pharm. 535, 379-392.

Jiang, G., Qin, X., 2014. An improved free surface electrospinning for high throughput manufacturing of core–shell nanofibers. Mater. Lett. 128, 259-262.

Kang, S., Hou, S., Chen, X., Yu, D.-G., Wang, L., Li, X., R Williams, G., 2020. Energy-saving electrospinning with a concentric teflon-core rod spinneret to create medicated nanofibers. Polymers 12, 2421.

Kessick, R., Fenn, J., Tepper, G., 2004. The use of AC potentials in electrospraying and electrospinning processes. Polymer 45, 2981-2984.

Koller, D.M., Posch, A., Hörl, G., Voura, C., Radl, S., Urbanetz, N., Fraser, S.D., Tritthart, W., Reiter, F., Schlingmann, M., Khinast, J., 2011. Continuous quantitative monitoring of powder mixing dynamics by near-infrared spectroscopy. Powder Technol. 205, 87-96.

Kumar, A., Wei, M., Barry, C., Chen, J., Mead, J., 2010. Controlling fiber repulsion in multijet electrospinning for higher throughput. Macromol. Mater. Eng. 295, 701-708.

Kunnath, K., Huang, Z., Chen, L., Zheng, K., Davé, R., 2018. Improved properties of fine active pharmaceutical ingredient powder blends and tablets at high drug loading via dry particle coating. Int. J. Pharm. 543, 288-299.

Lawrence, X.Y., Kopcha, M., 2017. The future of pharmaceutical quality and the path to get there. Int. J. Pharm. 528, 354-359.

Levit, S.L., Stwodah, R.M., Tang, C., 2018. Rapid, room temperature nanoparticle drying and low-energy reconstitution via electrospinning. J. Pharm. Sci. 107, 807-813.

Liu, J., Su, Q., Moreno, M., Laird, C., Nagy, Z., Reklaitis, G., 2018. Robust state estimation of feeding–blending systems in continuous pharmaceutical manufacturing. Chem. Eng. Res. Des. 134, 140-153.

Markl, D., Warman, M., Dumarey, M., Bergman, E.-L., Folestad, S., Shi, Z., Manley, L.F., Goodwin, D.J., Zeitler, J.A., 2020. Review of real-time release testing of pharmaceutical tablets: State-of-the art, challenges and future perspective. International journal of pharmaceutics 582, 119353.

Martínez, L., Peinado, A., Liesum, L., Betz, G., 2013. Use of near-infrared spectroscopy to quantify drug content on a continuous blending process: influence of mass flow and rotation speed variations. Eur. J. Pharm. Biopharm. 84, 606-615.

Masters, K., 1985. Spray drying handbook. Spray drying handbook.

Mullarney, M.P., Beach, L.E., Davé, R.N., Langdon, B.A., Polizzi, M., Blackwood, D.O., 2011. Applying dry powder coatings to pharmaceutical powders using a comil for improving powder flow and bulk density. Powder Technol. 212, 397-402.

Nagy, B., Farkas, A., Borbás, E., Vass, P., Nagy, Z.K., Marosi, G., 2019. Raman spectroscopy for process analytical technologies of pharmaceutical secondary manufacturing. AAPS PharmSciTech 20, 1.

Nagy, B., Farkas, A., Gyürkés, M., Komaromy-Hiller, S., Démuth, B., Szabó, B., Nusser, D., Borbás, E., Marosi, G., Nagy, Z.K., 2017. In-line Raman spectroscopic monitoring and feedback control of a continuous twin-screw pharmaceutical powder blending and tableting process. Int. J. Pharm. 530, 21-29.

Nagy, Z.K., Balogh, A., Démuth, B., Pataki, H., Vigh, T., Szabó, B., Molnár, K., Schmidt, B.T., Horák, P., Marosi, G., Verreck, G., Van Assche, I., Brewster, M.E., 2015. High speed electrospinning for scaled-up production of amorphous solid dispersion of itraconazole. Int. J. Pharm. 480, 137-142.

Nagy, Z.K., Balogh, A., Vajna, B., Farkas, A., Patyi, G., Kramarics, Á., Marosi, G., 2012. Comparison of electrospun and extruded Soluplus®-based solid dosage forms of improved dissolution. Journal of pharmaceutical sciences 101, 322-332.

Pandi, P., Bulusu, R., Kommineni, N., Khan, W., Singh, M., 2020. Amorphous solid dispersions: An update for preparation, characterization, mechanism on bioavailability, stability, regulatory considerations and marketed products. Int. J. Pharm., 119560.

Pharma, J., 2016. Benefits of using high functionality excipients in a continuous manufacturing process.

Pharmacopeia, U.S., 2007. Uniformity of Dosage Units.

Pingali, K.C., Saranteas, K., Foroughi, R., Muzzio, F.J., 2009. Practical methods for improving flow properties of active pharmaceutical ingredients. Drug development and industrial pharmacy 35, 1460-1469.

Sipos, E., Kósa, N., Kazsoki, A., Szabó, Z.-I., Zelkó, R., 2019. Formulation and characterization of aceclofenac-loaded nanofiber based orally dissolving webs. Pharmaceutics 11, 417.

Sóti, P.L., Bocz, K., Pataki, H., Eke, Z., Farkas, A., Verreck, G., Kiss, É., Fekete, P., Vigh, T., Wagner, I., Nagy, Z.K., Marosi, G., 2015. Comparison of spray drying, electroblowing and electrospinning for preparation of Eudragit E and itraconazole solid dispersions. Int. J. Pharm. 494, 23-30.

Szabó, E., Démuth, B., Galata, D.L., Vass, P., Hirsch, E., Csontos, I., Marosi, G., Nagy, Z.K., 2019. Continuous formulation approaches of amorphous solid dispersions: Significance of powder flow properties and feeding performance. Pharmaceutics 11, 654.

Szabó, E., Démuth, B., Nagy, B., Molnár, K., Farkas, A., Szabó, B., Balogh, A., Hirsch, E., Nagy, B., Marosi, G., Nagy, Z., 2018. Scaled-up preparation of drug-loaded electrospun polymer fibres and investigation of their continuous processing to tablet form. Express Polym. Lett. 12, 436-451.

Van Snick, B., Dhondt, J., Pandelaere, K., Bertels, J., Mertens, R., Klingeleers, D., Di Pretoro, G., Remon, J.P., Vervaet, C., De Beer, T., 2018. A multivariate raw material property database to facilitate drug product development and enable in-silico design of pharmaceutical dry powder processes. International journal of pharmaceutics 549, 415-435.

Vanarase, A.U., Alcalà, M., Rozo, J.I.J., Muzzio, F.J., Romañach, R.J., 2010. Real-time monitoring of drug concentration in a continuous powder mixing process using NIR spectroscopy. Chem. Eng. Sci. 65, 5728-5733.

Vanarase, A.U., Osorio, J.G., Muzzio, F.J., 2013. Effects of powder flow properties and shear environment on the performance of continuous mixing of pharmaceutical powders. Powder Technol. 246, 63-72.

Vanhoorne, V., Van Bockstal, P.-J., Van Snick, B., Peeters, E., Monteyne, T., Gomes, P., De Beer, T., Remon, J.P., Vervaet, C., 2016. Continuous manufacturing of delta mannitol by cospray drying with PVP. International journal of pharmaceutics 501, 139-147.

Vass, P., Démuth, B., Farkas, A., Hirsch, E., Szabó, E., Nagy, B., Andersen, S.K., Vigh, T., Verreck, G., Csontos, I., Marosi, G., Nagy, Z.K., 2019a. Continuous alternative to freeze drying: Manufacturing of cyclodextrin-based reconstitution powder from aqueous solution using scaled-up electrospinning. J. Control. Release 298, 120-127.

Vass, P., Hirsch, E., Kóczián, R., Démuth, B., Farkas, A., Fehér, C., Szabó, E., Németh, Á., Andersen, S.K., Vigh, T., Verreck, G., Csontos, I., Marosi, G., Nagy, Z.K., 2019b. Scaled-up production and tableting of grindable electrospun fibers containing a protein-type drug. Pharmaceutics 11, 329.

Vass, P., Szabó, E., Domokos, A., Hirsch, E., Galata, D., Farkas, B., Démuth, B., Andersen, S.K., Vigh, T., Verreck, G., Marosi, G., Nagy, Z.K., 2019c. Scale- up of electrospinning technology: Applications in the pharmaceutical industry. Wiley Interdiscip. Rev. Nanomed. Nanobiotechnol., e1611.

Vergote, G., De Beer, T., Vervaet, C., Remon, J.P., Baeyens, W., Diericx, N., Verpoort, F., 2004. In-line monitoring of a pharmaceutical blending process using FT-Raman spectroscopy. Eur. J. Pharm. Sci. 21, 479-485.

Williams, H.D., Trevaskis, N.L., Charman, S.A., Shanker, R.M., Charman, W.N., Pouton, C.W., Porter, C.J., 2013. Strategies to address low drug solubility in discovery and development. Pharmacological reviews 65, 315-499.

Yu, D.-G., Li, J.-J., Williams, G.R., Zhao, M., 2018. Electrospun amorphous solid dispersions of poorly water-soluble drugs: A review. J. Control. Release 292, 91-110.